Original Research

T_1 Mapping Using Variable Flip Angle SPGR Data With Flip Angle Correction

Gilad Liberman, MS,[1,2] Yoram Louzoun, PhD,[2,3] and Dafna Ben Bashat, PhD[1,4]*

Purpose: To improve the calculation of T_1 relaxation time from a set of variable flip-angle (FA) spoiled gradient recalled echo images.

Materials and Methods: The proposed method: (a) uses a uniform weighting of all FAs, (b) takes into account global inaccuracies in the generation of the prescribed FAs by estimating the actual FAs, and (c) incorporates data-driven local B_1 inhomogeneity corrections. The method was validated and its accuracy tested using simulated data, phantom, and in vivo experiments. Results were compared with existing analysis methods and to inversion recovery (IR). Consistency was assessed by means of repeated scans of two subjects. Reference values were obtained from eight healthy subjects from various brain regions and compared with literature values.

Results: The method accurately and consistently estimated T_1 values in all cases. The method was more robust, in comparison with the standard method, to the choice of FA set; to inaccuracies in generation of the prescribed FAs (in simulated data, T_1 estimation error was 12.1 ms versus 235.5 ms); demonstrated greater consistency (in vivo study showed interscan T_1 difference of 80 ms versus 356 ms); and achieved a better agreement with IR on phantom (median absolute difference of 123.8 ms versus 790 ms). Reference T_1 values were 883/801 ms for female/male in white matter and 1501/1349 ms in gray matter, within the range previously reported.

Conclusion: The proposed method overcomes some inaccuracies in FA production, providing more accurate estimation of T_1 values compared with standard methods, and is applicable for currently available data.

Key Words: relaxometry; T_1 mapping; FA correction, SPGR
J. Magn. Reson. Imaging 2014;40:171–180.

ACCURATE ESTIMATION OF the longitudinal relaxation time, T_1, of brain tissues has multiple clinical applications, and plays a significant role in the shift toward quantitative analysis of MRI signals. In clinical research of several neurological disorders, such as multiple sclerosis and Parkinson's disease (1,2), T_1 values improve the delineation of specific brain structures and the differentiation between patients and healthy subjects. In addition, accurate T_1 values are necessary for the extraction of pharmacokinetic parameters, from dynamic contrast enhanced (DCE) data (3). Additionally, knowledge of the T_1 value leads to better approximation of the T_2 value in certain methods, such as driven equilibrium single pulse observation of T_2 (DESPOT2) (4).

To this end, various MRI sequences and analysis methods have been proposed to calculate the T_1 value (4–11). One of these methods is the variable flip-angle (VFA) spoiled gradient recalled echo (SPGR) method, that provides high spatial resolution with relatively short acquisition times (1,4), and is commonly used in basic and clinical research. Significant efforts have been devoted to developing a fast and highly accurate analysis (12) of the VFA-SPGR data and to finding the best set of flip angles (FAs) that maximize accuracy and efficiency (in terms of T_1 value to noise ratio per acquisition time unit), for a specific T_1 value or a range of values (4,13,14). There is currently no broadly accepted FA set, and in many institutions, a varied set of angles is used. In addition, most current methods weight each FA dataset by a different factor that depends on the FA, resulting in a nonuniform weighting of the datasets. Thus, the calculated maps are affected by the choice of the FA set (13).

Another limitation of most current analysis methods is that they base their calculation of the T_1 values on the prescribed FA as reported by the MRI system. Yet, the actual FA might deviate from the one reported by the system, both globally, which may occur due to inaccuracy in calibration, and locally, due to inhomogeneity in the radiofrequency (RF) transmit field B_1. Several sequences have been proposed to determine

[1]The Functional Brain Center, The Wohl Institute for Advanced Imaging, Tel Aviv Sourasky Medical Center, Tel Aviv, Israel.
[2]Gonda Multidisciplinary Brain Research Center, Bar-Ilan University, Ramat Gan, Israel.
[3]Department of Mathematics, Bar-Ilan University, Ramat Gan, Israel.
[4]Sacklar Faculty of Medicine, Tel Aviv University, Tel Aviv, Israel.
Additional Supporting information may be found in the online version of this article.
Contract grant sponsor: James S. McDonnell Foundation; Contract grant number: 220020176.
*Address reprint requests to: D.B.B., The Wohl Institute for Advanced Imaging, Brain Imaging Center, Tel Aviv Sourasky Medical Center, 6 Weizmann Street, Tel Aviv, 64239, Israel. E-mail: dafnab@tlvmc.gov.il
Received February 28, 2013; Accepted July 14, 2013.
DOI 10.1002/jmri.24373
View this article online at wileyonlinelibrary.com.

the B_1 inhomogeneity (5,15,16), with the aim of improving the precision of the T_1 value estimate (5). An approximation formula and analysis of T_1 error due to B_1 inhomogeneities have been separately devised (17). Several sequences have been developed for actual FA imaging (AFI) (16,18) which use SPGR with multiple repetition times (TRs) and multiple FAs, to measure the actual FA along with T_1 mapping. However these methods are not always available in clinical systems, and do not deal with global inaccuracies in the production of the prescribed FAs, which are FA dependent.

In the present work, a new method to calculate T_1 values from the VFA-SPGR data is proposed with several advantages over existing methods: (i) the method weights the different FAs almost uniformly, resulting in a reduction of the error of fit; (ii) it estimates the global deviation from the prescribed FA due to inaccuracies in FA production, and by using the actual FAs, a better fit is obtained, not only in terms of error of fit, but also in the uniformity of the error of fit maps, indicating that the deviations from the prescribed FAs indeed stem from incorrect report of the actual FAs; and (iii) data-driven B_1 inhomogeneities correction is incorporated. The method proposed in this study works with the most commonly available data, acquired using VFA-SPGR, regardless of the way the calibration was performed and of the choice of the FA set. The accuracy and reproducibility of the method was compared with the standard method on simulated data, phantom and in vivo experiments. Finally, reference T_1 values of different brain areas of healthy subjects were obtained using the proposed method and compared with literature values.

MATERIAL AND METHODS

The Standard Method for Estimating the T_1 Value From VFA-SPGR Data

The signal S detected with an SPGR sequence depends on: the equilibrium longitudinal magnetization (M_0) which is related to the proton density; the repetition time TR; the T_1 value of the tissue; and the FA (α):

$$S = M_0 \cdot \frac{1-\exp(-\mathrm{TR}/T_1)}{1-\exp(-\mathrm{TR}/T_1)\cos(\alpha)}\sin(\alpha). \qquad [1]$$

Other multiplicative factors, such as T_2, T_2* and B_0 inhomogeneity effects are assumed to remain constant while the FA is changed. These factors will affect the estimation of M_0, but not of T_1. A common method to calculate the T_1 values from a given set of acquisitions with different FAs was suggested by Blüml (19), assuming constant TR values. In this method, a linear equation system is constructed, where each equation is a linearization of Eq. [1] for a different FA. The linearization is performed by multiplying Eq. [1] by $c_\alpha = (1-\exp(\text{-TR}/T_1)\cos(\alpha))/\sin(\alpha)$ and rearranging, resulting in:

$$\frac{S}{\sin(\alpha)} = \frac{S\cdot\exp(\text{-TR}/T_1)}{\tan(\alpha)} + M_0(1-\exp(-\mathrm{TR}/T_1)). \qquad [2]$$

Written in matrix form for different FAs, this becomes

$$\begin{pmatrix} \frac{S_1}{\sin(\alpha_1)} \\ \frac{S_2}{\sin(\alpha_2)} \\ \vdots \\ \frac{S_n}{\sin(\alpha_n)} \end{pmatrix} = \begin{pmatrix} \frac{S_1}{\tan(\alpha_1)} & 1 \\ \frac{S_2}{\tan(\alpha_2)} & 1 \\ \vdots & \vdots \\ \frac{S_n}{\tan(\alpha_n)} & 1 \end{pmatrix} \cdot \begin{pmatrix} \exp(-\mathrm{TR}/T_1) \\ M_0\cdot(1-\exp(-\mathrm{TR}/T_1)) \end{pmatrix}, \qquad [3]$$

where n is the number of FAs acquired. The resulting equation system [3] has a line form ($y_i = ax_i + b$), where the T_1 value can be simply extracted from the slope coefficient of this linear regression problem. We will refer to this method as the line fit method. Note that the line-fit method aims to fit Eq. [2], rather than Eq. [1]. As c_α is FA dependent, it is different for each instance of Eq. [2] in the equation system [3]. Thus it operates as a *weighting factor*, giving different weights for the different FA datasets, resulting in a suboptimal fit to the actual signal data.

The Proposed Method

Here, we propose three modifications to the method to improve the estimation of the T_1 value.

Uniform Weighting of All Flip Angles

Aiming for a linear equation with uniform weighting, we would like to have a new weighting coefficient c'_α to be only weakly dependent on α. As the numerator of c_α, $1-\exp(-\mathrm{TR}/T_1)\cos(\alpha)$, is used for the linearization, we change the denominator to be a good approximation of it, $1-\exp(-\mathrm{TR}/T_1')\cos(\alpha)$, where T_1' approximates the real T_1 value. This results in our weighting factor:

$$c'_\alpha = (1-\exp(-\mathrm{TR}/T_1)\cos(\alpha))/(1-\exp(-\mathrm{TR}/T_1')\cos(\alpha)) \approx 1, \forall\alpha \qquad [4]$$

which leads to the following equation system:

$$\begin{pmatrix} \frac{S_1}{1-\exp(-TR/T_1')\cos(\alpha_1)} \\ \frac{S_2}{1-\exp(-TR/T_1')\cos(\alpha_2)} \\ \vdots \\ \frac{S_n}{1-\exp(-TR/T_1')\cos(\alpha_n)} \end{pmatrix} = \begin{pmatrix} \frac{S_1\cos(\alpha_1)}{1-\exp(-TR/T_1')\cos(\alpha_1)} & \frac{1}{1-\exp(-TR/T_1')\cos(\alpha_1)} \\ \frac{S_2\cos(\alpha_2)}{1-\exp(-TR/T_1')\cos(\alpha_2)} & \frac{1}{1-\exp(-TR/T_1')\cos(\alpha_2)} \\ \vdots & \vdots \\ \frac{S_n\cos(\alpha_n)}{1-\exp(-TR/T_1')\cos(\alpha_n)} & \frac{1}{1-\exp(-TR/T_1')\cos(\alpha_n)} \end{pmatrix} \cdot \begin{pmatrix} \exp(-TR/T_1) \\ M_0\cdot(1-\exp(-TR/T_1)) \end{pmatrix}, \qquad [5]$$

A linear equation system which can be solved with the same complexity as the standard method. In this case, T_1' needs to be defined. It can be predefined to an accepted value detected in the brain, eg, 1200 ms. Note that this is a constant and a priori known value, and thus does not harm linearity. An additional iteration is performed to optimize this value, where T_1' used in the second iteration is the T_1 value calculated in the previous step. For a wide range of T_1 values (300–2500 ms), two iterations were found to be enough for convergence, leading to $c'_\alpha \approx 1$, for any reasonable α. We will refer to these stages of analysis as the one- and two-step methods, respectively (for pseudo-code, see Supp. Material S1, which is available online).

Estimation of the Actual Flip Angles

Actual FAs can vary from prescribed ones. Using linear approximations and the half-angle substitution, Helms et al (17) derived a simple approximation to Eq. [1]: as:

$$S \cong M_0 \alpha \frac{TR/T_1}{\alpha^2/2 + TR/T_1}. \qquad \text{[6, Eq. 7 in (15)]}$$

The T_1' and M_0' resulting from local inhomogeneity in B_1, i.e., dividing all of the FAs by a constant factor to be $\alpha\prime \cong \alpha/k$ are as follows:

$$T_1' \cong T_1 \cdot k^2, \quad M_0' \cong M_0 \cdot k. \quad \text{[7a,b, Eq. 11a,b in (15)]}$$

The signal of a voxel with these parameters and the FA affected by the B_1 inhomogeneity will be as follows:

$$\begin{aligned} S' &\cong M_0' \alpha' \frac{TR/T_1'}{\alpha\prime^2/2 + TR/T\prime_1} \\ &= (M_0 \cdot k)(\alpha/k) \frac{TR/(T_1 \cdot k^2)}{\alpha^2/(2k^2) + TR/(T_1 \cdot k^2)} \\ &= M_0 \alpha \frac{TR/T_1}{\alpha^2/2 + TR/T_1} \cong S. \end{aligned} \qquad [8]$$

thus, the changes in the T_1 and M_0 values completely compensate at the signal level for the constant multiplicative change in the FA, for any of the FAs, and the two configurations are indistinguishable in VFA-SPGR data at the voxel level. This claim was also numerically validated. Thus using the prescribed FAs in the calculation will lead to inaccuracy in the T_1 estimation, while the error of fit in the equation system (ie, either [3] or [5]) will be insignificant.

However, if each FA deviates from its prescribed value differently, using the prescribed values will result in both inaccuracy in the T_1 estimation and in a significant error of fit (due to the fact that the 2 free parameters, T_1 and M_0, cannot capture the higher dimensional space spanned by the FA deviations, assuming more than 2 FAs).

We suggest a *search* in the FA additive deviation space to minimize the error of fit. As a consistent multiplicative change in the FAs does not affect the error of fit, one degree of freedom is reduced by fixing one of the FAs to some value (eg, in this study, the median FA to its prescribed value). In other words, we propose a *search* in the (*n-1*)-dimensional space for deviation from the prescribed FAs, where *n* is the number of FAs given, while keeping one FA fixed. The optimization problem can be formalized as:

$$\Theta^* = (d_1, \cdots, d_{n-1}) = \arg\min_\Theta \left(\sum_{v \in Samples} RMS_v(\vec{S_v}, \Theta) \right) \qquad [9]$$

where $\vec{S_v}$ is the vector of *n* VFA-SPGR signal values corresponding to the acquisition in the voxel *v*, and $RMS_v(\vec{S_v}, \Theta)$ is the root-mean-square error of fit criteria between $\vec{S_v}$ and a signal simulated using the FAs with deviations Θ (where, for each Θ evaluated during the search, the T_1 and M_0 values used are the ones found by the two-step method presented above (Pseudo-code is provided in S2).

This part of the method is insensitive to local inhomogeneity, which appears as a constant multiplicative change in the FAs (eg, the effective value for all of the FA in a specific voxel might be 70% of their global value). Therefore, compensation for B_1 inhomogeneity is applied, as described next.

B_1 Inhomogeneity Correction

In the last step, a data-driven extraction of the change in the *localized* actual FA, due to the B_1 inhomogeneity, is proposed. Data-driven B_1 inhomogeneity correction algorithms are based on various assumptions. The N3 algorithm (20) presupposes: (a) a smooth multiplicative field, and (b) smoothing of an originally multimodal histogram which results from the field (formally described as reduction of the high frequency content of the intensity distribution). These hold for the T_1 map: (a) as can be seen by the approximation developed by Helms et al (17) (see Eq. 7a here), a multiplicative change in the FA values leads to an approximately inverse squared multiplicative change in the T_1 value. Thus the B_1 field is reflected in the T_1 map as a smooth multiplicative field. (b) The real T_1 value histogram is expected to contain distinct peaks corresponding to the various tissues.

Given that these two assumptions hold, we propose to apply the N3 algorithm to the calculated T_1 map, rather than to the raw data. This gives more accurate T_1 values, by correcting for the B_1 inhomogeneity, without the need for additional scans (for pseudo-code, see S3).

Note that the inhomogeneity estimation is true up to a global multiplicative factor (eg, it estimates that the field in voxel *a* is 20% weaker than in voxel *b*, but it does not tell if we should thus compensate the value in *a* accordingly, leave it as it is and compensate the value in *b*, or compensate both to some degree). Therefore, a global multiplicative factor is chosen such that it fixes a value at a given region of interest (ROI) to an a priori known value (in this study, the value of the white matter (WM) was set to 830 ms) (21).

Validation of the Method and Obtaining Reference Values

Simulated Data

Dataset 1

VFA-SPGR signals were simulated using Eq. [1], with TR = 5.6 ms, M_0 = 10,000 (a.u.), FAs in the range

[2–50]°, and several T_1 values: 300, 1200, and 2500 ms. For the two-step method, the FA set used was {2, 9, 20}° and Gaussian noise with $\sigma = 30$, corresponding to a signal to noise ratio (SNR) of around 10, was added to the data. These data were used to calculate the weights on the different FAs using the proposed method, in comparison to the line fit method.

Dataset 2

The three-dimensional (3D) VFA-SPGR images were simulated using M_0 and T_1 values obtained from a healthy subject for the FA set {1.4, 2.6, 4.8, 7.8, 13.3, 15.1, 17.6}°. These M_0, T_1 maps and FA values will be referred to as "actual." The related "prescribed" FAs given to the algorithm were {2, 3, 5, 9, 16, 20, 25}°. A Gaussian noise with $\sigma = 10$ was added, a realistic standard deviation in our data. These data were used to assess the method's accuracy in estimating the actual FAs.

Phantom Data

A phantom of a chicken leg was scanned using inversion recovery (IR) with inversion time TI = {200, 500, 1000, 1400, 3000}ms and TR/TE = 10000/13 ms, and with VFA-SPGR with FA set {2, 10, 15, 20, 30}° and TR/TE = (5.64 to 5.82)/2.1 ms. The data were used to test the accuracy of the suggested method. The VFA-SPGR data were analyzed twice, using the standard and the proposed methods. Errors of fit measurements are presented for voxels for which the signal was above 100 (a.u.) in all FA datasets. Comparison to IR were done after reslicing into the IR space, on a mask containing voxels for which all of the IR signals were above 100 (a.u.), and eroded by a disk kernel of 11 voxels radius to exclude margin effects.

In Vivo Experiment

Ten healthy subjects were scanned on a 3 Tesla (T) GE HDxt scanner (GE Signa EXCITE, Milwaukee, WI, USA) using 3D FSPGR sequences, with separate calibration for each FA acquisition.

Subjects were scanned using head quad coil, with field of view (FOV)/ acquisition matrix: 24 × 18 cm/ 256 × 128, bandwidth of 31.25 kHz, slice thickness of 5 mm and two averages, unless otherwise specified. Scan time (for each FA) was in the range of 12–38 s depending on the number of slices acquired.

One subject (subject number 1; male) was scanned using the FA set {2, 3, 5, 8, 10, 12, 2, 3, 5, 8, 10, 12, 15, 18, 25}° with repetition time/echo time (TR/TE) = 5.86/2.1 ms. This subject was scanned with an 8 channel head coil, acceleration factor of 2 and slice thickness of 4mm. These data were used to evaluate the inaccuracy in prescribed FA production.

One subject (subject number 2; male) was scanned twice, on 2 consecutive days, with an eight-channel head coil, acceleration factor of 2 and slice thickness of 5 mm using the FA set {3, 5, 12, 20}° with TR/TE = 5.56/1.61 ms on the first day and TR/TE = 5.768/ 1.65 ms on the second day. These data were used to test the consistency of the proposed method.

Eight subjects (five males, three females) were scanned using the FA set {3, 5, 12, 20}° with TR/TE = 4.96–5.55/1.57–2.1 ms. These data were used to obtain reference T_1 values from different brain areas. The study was approved by the Hospital's Institutional Review Board, and written informed consent was obtained from all subjects.

Data Analysis

T_1 values were calculated using the described two-step method, using the prescribed and actual FA values extracted by the method, and with and without B_1 correction using the N3 algorithm (20) applied to the resulting T_1 map. For validation of accuracy, results were compared between all analyses. For the healthy subjects' data, preprocessing included brain extraction performed using the BET module of the FSL toolbox (http://www.fmrib.ox.ac.uk/fsl) (22), and coregistration of all FA datasets of each subject was performed using the mutual-information criteria, to the median FA data, by SPM8's rigid coregistration module (23). When measuring the T_1 values in the various brain areas, the two-step method was used, using the extracted FAs with the B_1 inhomogeneity correction. The global multiplicative factor on the FAs was estimated by multiplying the T_1 map such that the mean value for WM ROIs would correspond to 830 ms, as reported by Wansapura et al (21).

Brain Area Definition

Several regions of interest (ROIs) were defined on the median FA volume to measure the T_1 values in the different brain areas. ROIs were defined in the same areas as in (21): frontal, parasagittal frontal, insular, parietal, parasagittal occipital and occipital gray matter (GM); frontal, parietal, and occipital WM and additionally in the corpus callosum and thalamus. The median T_1 values were calculated for each ROI in each subject to minimize partial volume and mislabeling effects. The average values of all eight subjects were calculated.

Minimization Procedure

The error of fit minimization in the FA deviation space was performed by running the Broyden-Fletcher-Goldfarb-Shanno algorithm (24) on several sample sets (10 sets of 1000 randomly chosen voxels), and choosing the corrected FA set which produced minimal error of fit for the *whole* volume (for pseudo-code, see S2).

Statistical Analyses

Statistical analyses were performed using MATLAB software (25). *t*-tests were performed to assess differences between maps obtained using the various methods. An analysis of variance (ANOVA) analysis was performed to assess the contribution of the prescribed FA value and subset chosen to the estimation of the FA, on all of the extracted FA values in Table 2.

RESULTS

The proposed method to analyze the VFA-SPGR data produced a more uniform weighting of the different FAs, as shown in the following subsection. By using the actual FAs, as estimated by the method, we obtained more accurate and consistent estimation of the T_1 values on the simulated data, on the phantom, and on consecutive scans of a healthy subject. Furthermore, we calculated T_1 values in various anatomical locations in healthy subjects and compared them with literature values, obtained using various acquisition and analysis methods, including IR. The comparison indicated a good agreement between our results and literature values.

Uniform Weighting of All Flip Angles

Simulated Dataset 1

The standard and suggested coefficients on S ($c_\alpha = (1 - \exp(-TR/T_1)\cos(\alpha))/\sin(\alpha)$ and $c'_\alpha = (1 - \exp(-TR/T_1)\cos(\alpha))/(1 - \exp(-TR/T'_1)\cos(\alpha))$, respectively) were calculated on simulated dataset 1. Figure 1 shows the weights on each FA data using the standard line-fit method (black), the suggested one-step method (blue, using $T_1' = 1200$ ms) and the two-step method (red). As can be seen, the weights using the two-step method are uniform for the whole range of FAs, for the full range of T_1 values tested. For example, for $T_1 = 1200$ ms, the 25° data are weighted ~2.4 times more than the 5° data using the line-fit method, while less than 5% more using the proposed two-step method. The coefficients in the proposed method are virtually independent of the FA. In our data, this step alone had a small effect on the T_1 estimation and the error of fit, yet the suggested mathematical elaboration may prove useful in devising better analyses.

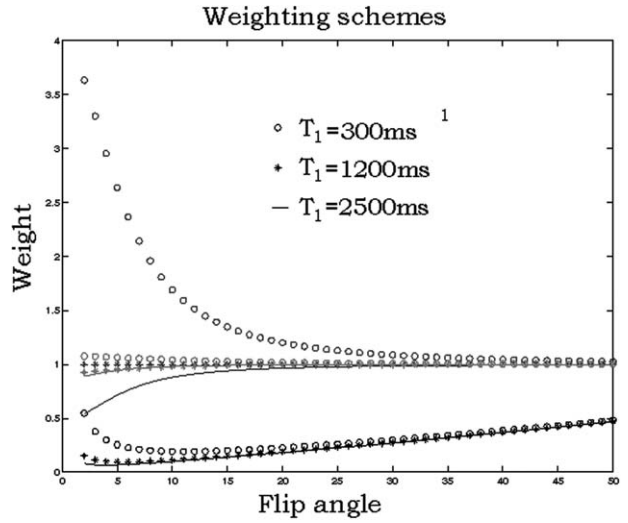

Figure 1. Weighting of the flip angle data: Black, using the commonly used line-fit weighting method. Blue, using the suggested one-step weighting method where $T_1' = 1200$ ms. Red, using the suggested two-step weighting method, using the T_1' from the first step.

Table 1
Effective vs. Extracted FA Values*

Effective	Extracted
1.40, 2.60, 4.80	1.46, 2.73, 5.33
1.40, 4.80, 13.30	1.40, 4.80, 13.32
1.40, 7.8,0 17.60	1.40, 7.77, 17.56
1.40, 4.80, 13.30, 17.60	**1.40, 4.80, 13.33, 17.62**
1.40, 2.60, 4.80, 13.30, 17.60	1.40, 2.61, 4.82, 13.30, 17.61
1.40, 4.80, 7.80, 15.10, 17.60	1.40, 4.80, 7.82, 15.10, 17.58
1.40, 4.80, 7.80, 13.30, 15.10, 17.60	1.40, 4.80, 7.81, 13.30, 15.10, 17.59
1.40, 2.60, 4.80, 7.80, 13.30, 15.10	1.40, 2.60, 4.81, 7.81, 13.30, 15.10 17.60

*The left column shows the effective FA values used for simulating MR signal. The right column shows the FA values extracted by the algorithm, when given the simulated signal and the corresponding nominal FAs from the set {2, 3, 5, 9, 16, 20, 25}.

Estimation of the Actual Flip Angles

Simulated Dataset 2

Several subsets of FAs, ie, different FA datasets, were taken from the full set {1.4, 2.6, 4.8, 7.8, 13.3, 15.1, 17.6}° of the simulated 3D MR images. The algorithm was initialized by the corresponding "prescribed" FA values: {2, 3, 5, 9, 16, 20, 25}°, and estimated values for the actual FAs were extracted by minimizing the error of fit on the data. The results are presented in Table 1. The extracted FAs were accurate in all cases except for minor deviation in the first subset, which included only small flip-angles.

T_1 maps were calculated using the "prescribed" {2, 5, 16, 25}° and extracted {1.40, 4.80, 13.33, 17.62}° FAs (from the fourth FA subset used, marked in bold in Table 1) and were compared with the T_1 map used for the simulation, calculated using the actual FAs. Figure 2 shows the real T_1 map (left), T_1 maps calculated using the "prescribed" FAs (top middle) and the extracted FAs (bottom middle) and their differences (right). The inaccuracies in T_1 estimation when using the "prescribed" FA values are significantly larger (mean absolute difference of 235.5 ms) and structured: the correlation between the T_1 difference map and the real T_1 map was high ($r = -0.99$; $P <$ 1e-10), indicating a consistent bias related to the T_1 value, ie, an incorrect model, rather than noise. The inaccuracies when using the extracted FA are smaller (mean absolute difference of 12.1 ms) and resemble uniform noise (with no correlation to the actual T_1 value, $r = -0.04$), indicating a full model of the signal up to the noise level.

In Vivo Experiment

The first subject was scanned with many prescribed FAs including some FAs that were repeated ({2, 3, 5, 8, 10, 12, 2, 3, 5, 8, 10, 12, 15, 18, 25}°). For several subsets of the data, we searched for the actual FAs by minimizing the error of fit. The prescribed and extracted FAs for several subsets of the data are shown in Table 2. The algorithm consistently extracted the same values independently of the FA subset used with only minor variations. In addition, different values were consistently extracted for

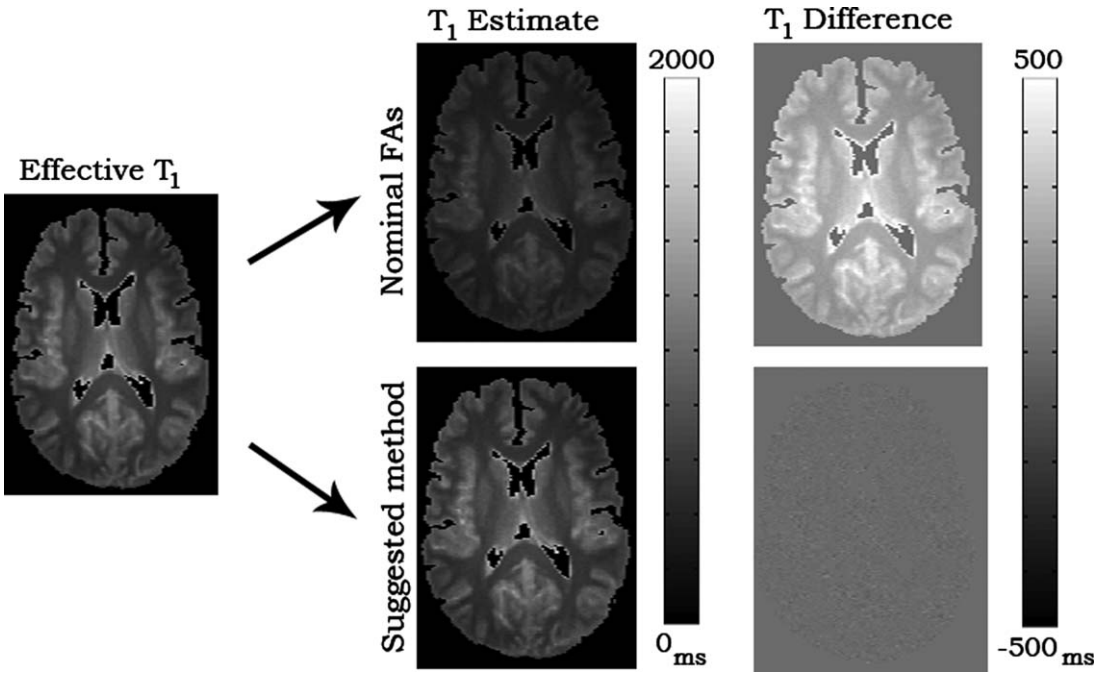

Figure 2. Estimation of the actual flip angles, simulated data. Left: The actual T_1 map used for the simulation. Middle: T_1 maps calculated using the "prescribed" FA values (top) and the extracted FA values (bottom). Right: The corresponding difference maps.

repeated acquisitions with the same prescribed values, for example, 11.62 ± 0.15 for 10^a and 10.10 ± 0.07 for 10^b. The method showed high consistency and robustness to the FA subset used. An ANOVA analysis on the actual FA values shows significance for prescribed FA value ($P < 1.e\text{-}10$) but not for the subset chosen ($P > 0.05$).

To confirm the finding that for the same prescribed FAs, the actual values were different; we focused on the fifth FA subset (marked in bold in Table 2). The mean absolute signal differences between the two acquisitions with the same prescribed FA were 53.16 (a.u.) for 10° and 65.06 (a.u.) for 2°. These large differences in the signal between two almost consecutive acquisitions of the same prescribed FA can be explained by the fact that different actual FAs were applied, as detected by the algorithm. Furthermore, images were simulated using the extracted FA values (11.65°, 10.04°, and 2.62°, 2.27°) based on the T_1 and M_0 maps obtained from this subject. These images were subtracted from the corresponding acquired MR images. Mean absolute differences were 10.49, 10.24 for 10^a,10^b and 4.76, 4.59 for 2^a,2^b (a.u., respectively). The smaller differences indicate that the simulation indeed captures the nature of the difference between the acquisitions, ie, the deviations from the prescribed FAs.

A similar analysis was performed on the data of the second subject, who was scanned twice on 2 consecutive days, with similar results; of note, the same prescribed FAs yielded different actual ones.

B_1 Inhomogeneity Correction and Consistency of T_1 Maps

In Vivo Experiment

Subject number 2 was scanned on 2 consecutive days with the same prescribed FAs. T_1 maps were calculated for each dataset using the standard method and the proposed method, using the extracted FAs and B_1 inhomogeneity correction, and the interscan differences were calculated (Fig. 3). Using the proposed method, the T_1 maps showed higher interscan consistency in comparison with the standard method (mean absolute difference between the T_1 maps of the 2 days: 80.8 ms and 356.7 ms, respectively); the interscan T_1 difference map was more uniform and lacked spatial anatomical structure. These results indicate that by accounting for inaccuracy in prescribed FA production and B_1 inhomogeneity, higher consistency in calculated T_1 maps can be achieved.

Accuracy of the Method

The phantom was scanned using both IR and VFA-SPGR and T_1 values were estimated from both datasets. T_1 value estimation from the VFA-SPGR data was performed using the standard and the proposed methods. Relative root-mean-square (rRMS, coefficient

Table 2
Nominal vs. Extracted Flip Angle Values for Subject 1*

Nominal					Extracted				
10^a	2^a	10^b	2^b	25	11.66	2.62	10.05	2.27	18.60
10^a	2^a	3	12	25	11.57	2.63	3.36	9.98	18.53
10^b	2^b	3	12	25	10.10	2.27	3.35	10.10	18.66
10^b	2^b	10^a	2^a	25	10.06	2.27	11.65	2.62	18.57
10^a	**2^a**	**10^b**	**2^b**	**25**	**11.65**	**2.62**	**10.04**	**2.27**	**18.58**
10^a	2^a	10^b	2^b		11.82	2.56	10.24	2.22	
10^a	2^a	25			11.37	2.67	18.36		
10^b	2^b	25			10.09	2.28	18.69		

*The left column shows the nominal flip angle values, as reported by the MRI system. The right column shows the flip angle values extracted by the method. Repeated acquisitions using the same flip angles are marked by superscript "a" and "b".

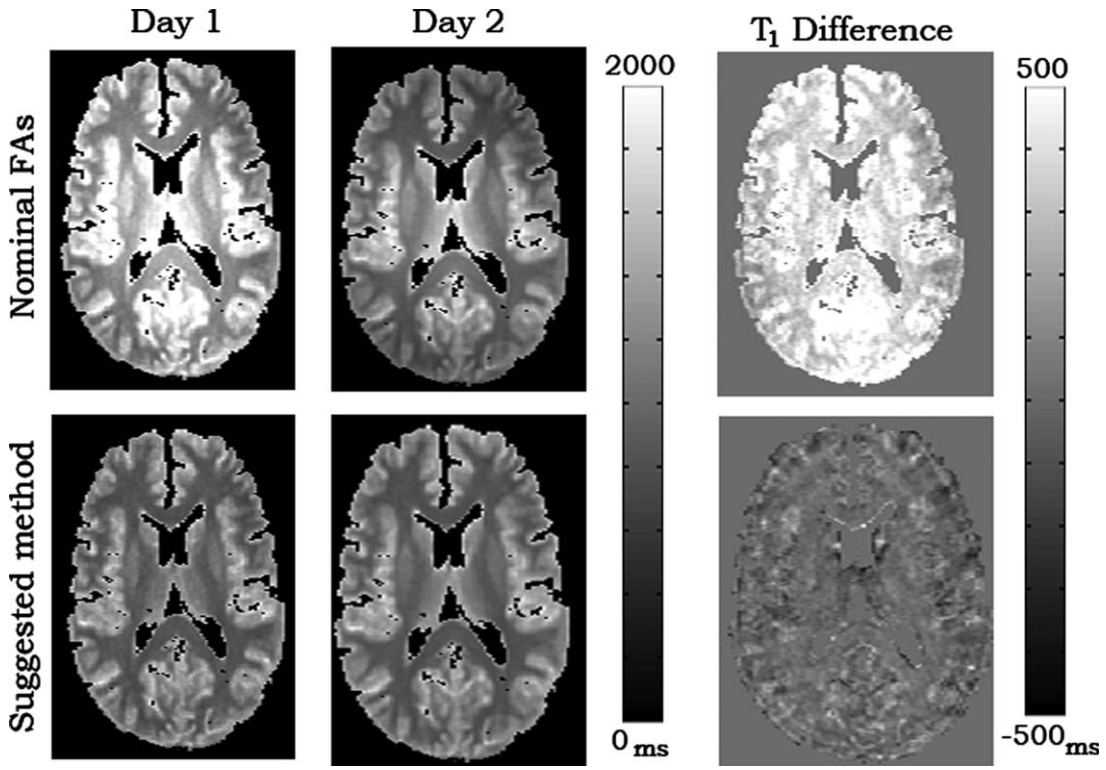

Figure 3. Consistency of T_1 maps. T_1 maps from both days, using the standard and the proposed methods, along with the corresponding interscan differences.

of variation of the RMS of the errors) values were calculated per voxel using both methods, with the results showing a much lower rRMS value using the actual FAs than using the standard method (mean rRMS of 0.01 versus 0.12, F-test *P*-value<1e-10). T_1 maps estimated from IR data (considered as gold-standard) and from the VFA-SPGR data using the standard and proposed methods, are presented in Figure 4a,b,c, along with the differences in T_1 estimation between IR and the two VFA-SPGR analyses (Fig. 4e,f). The proposed method achieved a better agreement with IR estimations (median absolute difference of 123.8 versus 790.0 ms). Note that similarly high differences to IR have been previously reported using the standard analysis method of VFA-SPGR on a 3T system (5). The proposed analysis overcomes much of this inaccuracy. Figure 4d shows a scatter plot of the T_1 values obtained using IR and VFA-SPGR with the suggested

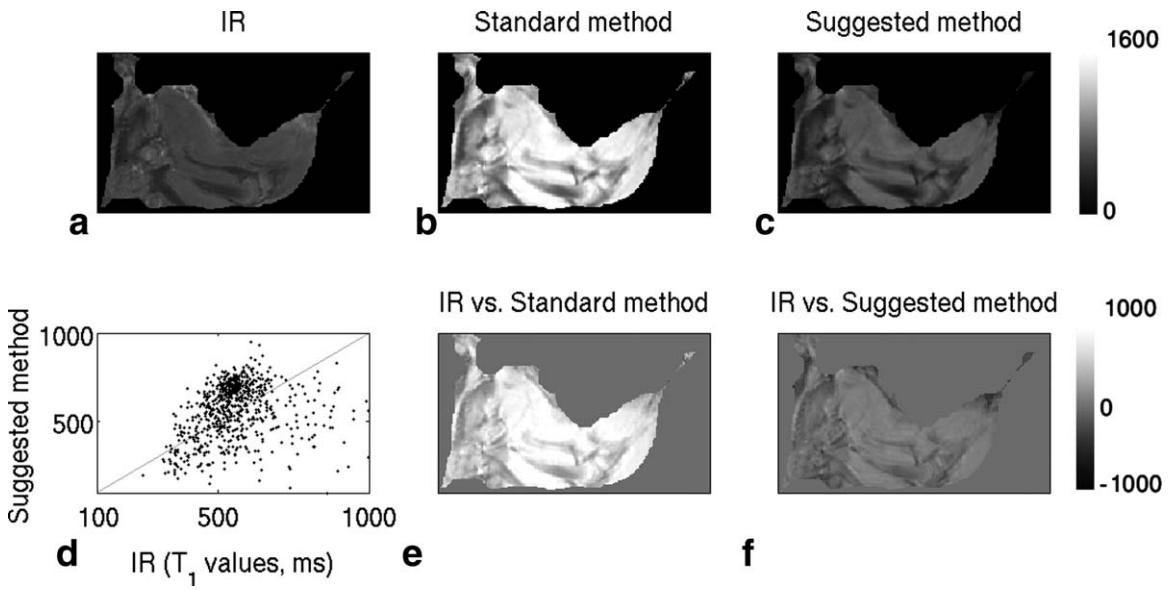

Figure 4. Accuracy of T_1 maps. T_1 maps estimated from IR and SPGR data (**a**) using the standard (**b**) and the proposed (**c**) methods, along with T_1 estimation difference maps between IR and the standard method (**e**), and IR and the proposed method (**f**). **d:** Scatter plot of the T_1 values estimated using IR and SPGR with the proposed method.

Table 3
T_1 Values (ms) Obtained in This Study in the Various Brain Tissues Compared to Literature

Reference	Method	Subjects	Blood[†] / CSF	WM	GM	Splenium	Thalamus	Other	Age (yr)
This study[‡]	VFA-SPGR - Proposed analysis	3 Females	6873 (CSF)	883	1501	1064	1699		
This study[‡]	VFA-SPGR - Proposed analysis	5 Males	4184 (CSF)	801	1349	906	1404		
Wansapura et al., 1999 (20)	* Saturation recovery	19 (8F, 11M)		832 (893 female, 788 male)	1331 (1393 female, 1286 male)				28–51, 29–47
Gelman et al., 2001 (27)	TOMROP	12 (7F, 5M)		847 (FWM)	1763 (PC)		1218	1147 (SN), 1043 (GP), 1337 (PT), 1483 (CN)	22–38
Chen et al., 2001 (25)	IR-FSE	10 (4F, 6M)	4163 (CSF)	791	1445		1271		31 ± 10
Ethofer et al., 2003 (26)	* Progressive saturation - MRS	8 (4F, 4M)		960 (FPWM), 1110 (OWM)				960 (CL), 1170 (M1), 1470 (OC)	19–34
Zhu and Penn, 2005 (31)	Adiabatic TESO-IR-FSE	12 (5F, 7M)		790, 761 (FWM), 791 (PWM)	1421	746, 724 (Genu)	1034	1129 (PT), 1190 (CN)	34 ± 9
Stanisz et al., 2005 (30)	IR	Bovine samples	1932b (Blood)	1084	1820				
Lu et al., 2005 (28)	aIR	10 (4F, 6M)		699 (FWM), 758 (OWM)	1209 (FGM)	748, 721 (Genu)	986	1102 (PT), 1122 (OC), 1258 (CN)	21–38
Cheng and Wright, 2006 (13)	VFA-SPGR + B1	2		1084, 1087	1703, 1732				
Rooney et al., 2007 (29)	Modified Look-Locker, estimated value for 3T.	3 (3M)	1961(Blood) 4300 (CSF)	887	1293 (IGM)				32–59
Deoni, 2007 (5)	VFA-SPGR+B1, IR; Analyzed by DESPOT1-HIFI, estimated from graph	3 (2F, 1M)		∼1060			∼1495	∼1230 (GP), ∼1570 (PT), ∼1610 (CN)	30,32, 26
Helms et al., 2008 (15)	FLASH, Two angles (7,20)	8 (4F, 4M)	4181(CSF)	801	1349	778		1408 (OC), 1269 (CN)	25–31

*Image of ROIs.
[†]and ref to ∼1550 Greenman 2003.
[‡]Note that the values were fixed such that WM value is the same as that reported by Wansapura, using the extra degree of freedom.
CC = corpus callosum; PC = prefrontal cortex; IGM = internal GM; OWM = occipital WM; FPWM = frontoparietal WM; M1 = motor cortex; CL = cerebellum; SN = substantia nigra; GP = globus pallidus,; PT = putamen; OC = occipital cortex; CN = head of the caudate nucleus.

method. While a good agreement was achieved, the correlation slope deviates from the 1:1 line (gray). This deviation might be the result of inaccuracies relating to IR measurements (such as incomplete inversion), and to the global factor on the B_1 inhomogeneity field.

Reference T_1 Values

T_1 maps were calculated in several brain areas of eight healthy subjects using the actual FAs, B_1 inhomogeneity correction and estimation of the consistent multiplicative coefficient. The values were normalized such that the mean WM ROIs value was set to 830 ms (as reported by Wansapura et al) (21), due to the extra degree of freedom related to the overall B_1 inhomogeneity coefficient. Note that this shift, ie, the effect of the overall amplitude of the B_1 inhomogeneity, is an inherent phenomenon, and not particular to the suggested analysis. In this study, the normalization resulted in a change of less than 5% in the T_1 values. Mean T_1 values in the various brain areas are presented in Table 3, along with literature values (5,13,17,21,26–32). The T_1 values, calculated using the proposed method, are within the interstudy range. The differences in T_1 values between male and female subjects detected in this study (see Table 3) support previous findings (21). Table 3 presents a comprehensive report of reference (3T) T_1 values measured in various studies. A large interstudy variability is evident, suggesting that true universal T_1 reference values for brain tissues are still unknown.

DISCUSSION

The current study proposed a method for calculating T_1 maps based on the commonly used VFA-SPGR method. This method weights the different FAs uniformly, uses corrected FAs rather than the prescribed FA values and corrects for B_1 inhomogeneity. The method shows high consistency in the actual FA value estimation regardless of the FA set used; in the calculation of T_1 maps in longitudinal scans; and higher accuracy than the standard method (33).

The problems considered in this study, ie, the biased weighting of the FA data, the inaccuracy in the production of the prescribed FA value and the overall amplitude of the B_1 field, are *inherent* to the VFA-SPGR acquisition, and many other acquisition methods. This study proposes an investigation of these parameters, usually perceived as fixed between acquisitions. Other factors, such as gain and baseline level, were investigated in a preliminary study and found to be unchanging during the VFA-SPGR acquisitions. This approach should be further applied to other sequences and analyses such as AFI mapping and T_2 measurements, and T_1 measurements through IR scans. Furthermore, we highlight the importance of the neglected error of fit maps for evaluation of the quality of a model.

When a single calibration is performed and applied to all FAs, their actual values may deviate by a constant multiplicative factor from the prescribed ones. However, when each acquisition is calibrated separately, the actual values may deviate by a different factor from the corresponding prescribed values. The proposed method is insensitive to both the choice of FA set and the calibration method used, not requiring any additional data such as B_1 mapping, and is therefore applicable to most available data. These advantages, in addition to the high accuracy and reproducibility, make the proposed method ideal for multi-center, longitudinal studies and applicable to retrospective data. While B_1 inhomogeneity is usually neglected in 1.5T systems, in 3T systems local changes in the actual FA due to B_1 inhomogeneity were shown to be significant (5). In this study, a data-driven algorithm was used to account for B_1 inhomogeneity, yet direct B_1 mapping methods, such as AFI (16), DESPOT1-HIFI (5), and DREAM (15) are recommended when available.

The approach of uniform weighting of the different FA data can be applied in other studies, to achieve a more accurate parameter estimation. Such schemes may give higher weights for specific data points (i.e., flip angle data) that were acquired with lower noise, or for which a greater a priori belief is assumed (for example, see Cheng and Wright) (13), with weights proportional to signal). Our weighting scheme does not contradict such considerations, but may serve as a basis for equalizing the weight of each data point before application.

Currently reported T_1 values obtained from healthy brain tissue show broad interstudy variation even between studies using the same or similar acquisition and analysis methods (5,13,17,21,26–32). This variability can result from the inaccuracy of the prescribed FA used, B_1 inhomogeneity and partial volume effect due to the ambiguity of ROI definition. Although our results showed general agreement with literature values, the variability between studies indicates that T_1 estimations should be currently considered as method-dependent, and maybe even system-, configuration-, and patient-group-dependent, rather that universal. By using the proposed method and selecting the median value for a set of several voxels (rather than the average of an area) for each ROI, more consistent and accurate T_1 values may be obtained.

Several limitations to the proposed method should be considered. The method uses data-driven analysis to estimate acquisition parameters for which a direct measurement is more accurate, indeed a direct measurement of the actual FA is preferable. For the B_1 inhomogeneity field mapping, several methods have been proposed (5,15,16) which are preferable when available. Another limitation is the need for a reference tissue with known T_1 value for normalization. However, we have shown that this limitation, while not always acknowledged, exists in other T_1 analysis methods, and is due to the system's inaccuracies, as detailed above, rather than being analysis-dependent.

In conclusion, we demonstrate that inaccuracies in production of the prescribed FAs may lead to significant T_1 estimation errors. We further propose a

method that can extract the actual FAs and compensate for these changes, as well as compensating for B_1 inhomogeneity effects and providing a more uniform weighting of the different FA data, leading to a more consistent and robust T_1 value estimation. A complete pseudo-code is presented in the supplementary material, and the source-code is available upon request. This method is widely applicable to currently available data, providing a valuable tool for accurate measurements of T_1 values.

ACKNOWLEDGMENTS

We thank Vicki Myers for editorial assistance and Moran Artzi and Faina Vitinshtein for assiting in data collection. D.B.B. was funded by the James S. McDonnell Foundation.

REFERENCES

1. Menke RA, Scholz J, Miller KL, et al. MRI characteristics of the substantia nigra in Parkinson's disease: a combined quantitative T1 and DTI study. Neuroimage 2009;47:435–441.
2. Stevenson VL, Parker GJM, Barker GJ, et al. Variations in T1 and T2 relaxation times of normal appearing white matter and lesions in multiple sclerosis. J Neurol Sci 2000;178:81–87.
3. O'Connor JPB, Jackson A, Parker GJM, Jayson GC. DCE-MRI biomarkers in the clinical evaluation of antiangiogenic and vascular disrupting agents. Br J Cancer 2007;96:189–195.
4. Deoni SCL, Rutt BK, Peters TM. Rapid combined T1 and T2 mapping using gradient recalled acquisition in the steady state. Magn Reson Med 2003;49:515–526.
5. Deoni SCL. High-resolution T1 mapping of the brain at 3T with driven equilibrium single pulse observation of T1 with high-speed incorporation of RF field inhomogeneities (DESPOT1-HIFI). J Magn Reson Imaging 2007;26:1106–1111.
6. Deoni SCL, Peters TM, Rutt BK. High-resolution T1 and T2 mapping of the brain in a clinically acceptable time with DESPOT1 and DESPOT2. Magn Reson Med 2005;53:237–241.
7. Henderson E, McKinnon G, Lee TY, Rutt BK. A fast 3D Look-Locker method for volumetric T1 mapping. Magn Reson Imaging 1999;17:1163–1171.
8. Messroghli DR, Radjenovic A, Kozerke S, Higgins DM, Sivananthan MU, Ridgway JP. Modified Look-Locker inversion recovery (MOLLI) for high-resolution T1 mapping of the heart. Magn Reson Med 2004;52:141–146.
9. Gowland P, Mansfield P. Accurate measurement of T1in vivo in less than 3 seconds using echo-planar imaging. Magn Reson Med 1993;30:351–354.
10. Graumann R, Deimling M, Heilmann T, Oppelt A. A new method for fast and precise T1 determination. Proc Soc Magn Reson Med 1986;1986:922–923.
11. Brix G, Schad LR, Deimling M, Lorenz WJ. Fast and precise T1 imaging using a TOMROP sequence. Magn Reson Imaging 1990; 8:351–356.
12. Wang HZ, Riederer SJ, Lee JN. Optimizing the precision in T1 relaxation estimation using limited flip angles. Magn Reson Med 1987;5:399–416.
13. Cheng H-LM, Wright GA. Rapid high-resolution T1 mapping by variable flip angles: accurate and precise measurements in the presence of radiofrequency field inhomogeneity. Magn Reson Med 2006;55:566–574.
14. Homer J, Roberts JK. Conditions for the driven equilibrium single pulse observation of spin-lattice relaxation times. J Magn Reson Imaging 1987;74:424–432.
15. Nehrke K, Börnert P. DREAM—a novel approach for robust, ultrafast, multislice B1 mapping. Magn Reson Med 2012;68:1517–1526.
16. Yarnykh VL. Actual flip-angle imaging in the pulsed steady state: a method for rapid three-dimensional mapping of the transmitted radiofrequency field. Magn Reson Med 2007;57:192–200.
17. Helms G, Dathe H, Dechent P. Quantitative FLASH MRI at 3T using a rational approximation of the Ernst equation. Magn Reson Med 2008;59:667–672.
18. Voigt T, Nehrke K, Doessel O, Katscher U. T1 corrected B1 mapping using multi-TR gradient echo sequences. Magn Reson Med 2010;64:725–733.
19. Blüml S, Schad LR, Stepanow B, Lorenz WJ. Spin-lattice relaxation time measurement by means of a TurboFLASH technique. Magn Reson Med 1993;30:289–295.
20. Sled JG, Zijdenbos AP, Evans AC. A nonparametric method for automatic correction of intensity nonuniformity in MRI data. IEEE Trans Med Imaging 1998;17:87–97.
21. Wansapura JP, Holland SK, Dunn RS, Ball WS. NMR relaxation times in the human brain at 3.0 tesla. J Magn Reson Imaging 1999;9:531–538.
22. Smith SM. Fast robust automated brain extraction. Hum Brain Mapp 2002;17:143–155.
23. Wells WMI, Viola P, Atsumi H, Nakajima S, Kikinis R. Multimodal volume registration by maximization of mutual information. Med Imaging Anal 1996;1:35–51.
24. Fletcher R.Modified marquardt subroutine for non-linear least squares. Atomic Energy Research Establishment 1971:AERE-R6799.
25. Guide MU. The MathWorks. Inc, Natick, MA 1998;5.
26. Chen L, Bernstein M, Huston J, Fain S.Measurements of T1 relaxation times at 3.0 T: implications for clinical MRA. In: Proceedings of the 9th Annual Meeting of ISMRM, Glasgow, Scotland, 2001. (abstract 1391).
27. Ethofer T, Mader I, Seeger U, et al. Comparison of longitudinal metabolite relaxation times in different regions of the human brain at 1.5 and 3 Tesla. Magn Reson Med 2003;50:1296–1301.
28. Gelman N, Ewing JR, Gorell JM, Spickler EM, Solomon EG. Interregional variation of longitudinal relaxation rates in human brain at 3.0 T: relation to estimated iron and water contents. Magn Reson Med 2001;45:71–79.
29. Lu H, Nagae-Poetscher LM, Golay X, Lin D, Pomper M, vanZijl PCM. Routine clinical brain MRI sequences for use at 3.0 Tesla. J Magn Reson Imaging 2005;22:13–22.
30. Rooney WD, Johnson G, Li X, et al. Magnetic field and tissue dependencies of human brain longitudinal 1H2O relaxation in vivo. Magn Reson Med 2007;57:308–318.
31. Stanisz GJ, Odrobina EE, Pun J, et al. T1, T2 relaxation and magnetization transfer in tissue at 3T. Magn Reson Med 2005;54: 507–512.
32. Zhu DC, Penn RD. Full-brain T1 mapping through inversion recovery fast spin echo imaging with time-efficient slice ordering. Magn Reson Med 2005;54:725–731.
33. Bagher-Ebadian H, Jain R, Nejad-Davarani SP, et al. Model selection for DCE-T1 studies in glioblastoma. Magn Reson Med 2012; 68:241–251.